

# A Kinematic Model of Wave Propagation

John W. Cain<sup>1</sup>

<sup>1</sup>Dept. of Mathematics, Virginia Commonwealth University,  
1001 W. Main Street, Richmond, Virginia, 23284-2014, USA  
e-mail: jwcain@vcu.edu

August 21, 2008

## Abstract

We present a purely kinematic model of wave propagation in an excitable medium, namely cardiac tissue. The kinematic model is constructed from a standard reaction-diffusion model, using asymptotic techniques to track the position and velocity of each propagating wave front and wave back. The kinematic model offers a substantial improvement in computational efficiency without sacrificing the ability to predict the onset of certain arrhythmias. Moreover, the linearized kinematic model equations can be solved exactly in terms of generalized Laguerre polynomials, allowing us to extract valuable physiological information.

**AMS Subject Classification:** 92C50, 33C45, 92C30

**Key Words and Phrases:** cardiac fiber, pacing, restitution, kinematic model, generalized Laguerre polynomials

## 1 Introduction

Traditionally, the mathematical study of cardiac arrhythmias has involved the use of reaction-diffusion systems to model propagation of the electrical waves that drive the beating of the heart. Such models govern the evolution of many physiological variables and, as a consequence, simulations can be computationally expensive. However, certain mechanisms for the onset of arrhythmias can be well-understood by simply tracking the progress of each propagating wave. In this paper, we provide a detailed example of how one may derive a computationally efficient kinematic model [7] of wave propagation, starting from a standard reaction-diffusion system. For detailed references, including a list of recent studies using kinematic models, see [1].

We shall require some terminology from cardiac electrophysiology, referring the reader to Figure 1 for an illustration of the following definitions. An *action potential* is a prolonged elevation of the voltage  $v$  across the cardiac cell membrane in response to an electrical stimulus. *Pacing* refers to repeated electrical

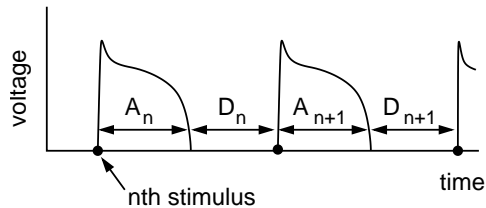


Figure 1: Voltage trace of several action potentials in a paced cardiac cell.

stimulation of cardiac tissue. *Action potential duration (APD)* is the amount of time in which the voltage  $v$  remains larger than a specified threshold  $v_{\text{thr}}$  after a cell is stimulated. The *diastolic interval (DI)* is the amount of time in which  $v < v_{\text{thr}}$  between consecutive action potentials. We shall denote the APD following the  $n^{\text{th}}$  stimulus by  $A_n$  and the subsequent DI by  $D_n$  (Figure 1).

In spatially extended tissue, electrical coupling of neighboring cells allows action potentials to propagate through the tissue [4]. Here, we shall model the dynamics of an idealized, paced cardiac fiber composed of cylindrical cells joined together in an end-to-end fashion. Assuming that voltage exhibits negligible radial dependence, varying only as a function of a length variable  $x$ , we may regard the fiber as one-dimensional. We assume that periodic pacing is performed locally at one end of the fiber which we identify with  $x = 0$ . To emphasize that both DI and APD may depend upon  $x$ , we shall write  $D_n(x)$  and  $A_n(x)$ .

## 2 Deriving the kinematic model

In this section, we show how a kinematic model of wave propagation can be derived from a standard reaction-diffusion model. In what follows, we consider a homogenous, one-dimensional fiber of length  $L$ . We assume that time is measured in milliseconds (ms) and distance is measured in centimeters (cm).

### 2.1 A two-variable reaction-diffusion model

One of the simplest models of the cardiac action potential is due to Mitchell and Schaeffer [5]. Their model consists of two dynamic variables: voltage  $v = v(x, t)$  and a generalized conductance  $h = h(x, t)$ , both of which are assumed to be non-dimensionalized and scaled to vary between 0 and 1. The equations are

$$\frac{\partial v}{\partial t} = \kappa \frac{\partial^2 v}{\partial x^2} + \frac{h}{\tau_{\text{in}}} v^2 (1 - v) - \frac{v}{\tau_{\text{out}}} + J_{\text{stim}}, \quad (1)$$

$$\frac{\partial h}{\partial t} = \left( \frac{1 - h}{\tau_{\text{open}}} \right) \Theta(v_{\text{crit}} - v) - \left( \frac{h}{\tau_{\text{close}}} \right) \Theta(v - v_{\text{crit}}), \quad (2)$$

where  $0 < x < L$  and Neumann boundary conditions are imposed. Here  $\Theta$  denotes the Heaviside function, and  $J_{\text{stim}}$  is a periodic (period  $B$ ) stimulus current applied at the  $x = 0$  end of the fiber. Generally, the time constants  $\tau_{\text{in}}$ ,  $\tau_{\text{out}}$ ,  $\tau_{\text{open}}$  and  $\tau_{\text{close}}$  are measured in milliseconds (ms), while the diffusion coefficient  $\kappa$  has units of  $\text{cm}^2/\text{ms}$ . The parameter  $v_{\text{crit}}$  represents a critical voltage, above which the cell reduces the flow of inward current. Sample parameter values appear in [2].

## 2.2 Restitution and dispersion functions

As the pacing period  $B$  is shortened, the corresponding steady-state APD decreases. This feature of cardiac tissue, known as electrical *restitution*, is key in the development of the kinematic model (see next subsection). Mathematically, restitution can be modeled with a one-dimensional mapping [6]

$$A_{n+1} = f(D_n) = f(B - A_n), \quad (3)$$

where  $f$  is known as the restitution function. As shown in [5], deriving a restitution function for the model (1)–(2) is similar in spirit to the derivation of a Poincaré mapping. To leading-order in  $\epsilon = \tau_{\text{out}}/\tau_{\text{close}}$ ,

$$f(DI) \sim \tau_{\text{close}} \ln \left[ \frac{h(DI)}{h_{\text{min}}} \right], \quad (4)$$

where

$$h(DI) = 1 - \left( 1 - \frac{4\tau_{\text{in}}}{\tau_{\text{out}}} \right) e^{-DI/\tau_{\text{open}}}. \quad (5)$$

The next-order correction to (4) is calculated in [2].

Like APD, the wave front velocity of an action potential also depends upon the preceding (local) DI. The analogue of the restitution function is called the dispersion function, and will be denoted by  $c(DI)$ . In [3], it is shown that a leading-order approximation of the dispersion function for (1)–(2) is given by

$$c(DI) = \max \left\{ \left[ \frac{1}{2} V_+(DI) - V_-(DI) \right] \sqrt{\frac{2\kappa h(DI)}{\tau_{\text{in}}}}, 0 \right\}, \quad (6)$$

where

$$V_{\pm}(DI) = \frac{1}{2} \left( 1 \pm \sqrt{1 - \frac{4\tau_{\text{in}}}{\tau_{\text{out}} h(DI)}} \right). \quad (7)$$

We remark that  $f(DI)$  has units of ms and  $c(DI)$  has units of cm/ms. With formulas (4) and (6), we now have enough information to track the position and velocity of each propagating wavefront and waveback.

### 2.3 Kinematic model of wave propagation

The restitution and dispersion functions specify the duration and velocity of each action potential as a function of the local DI, providing precisely the information we need to track all wave fronts and wave backs in a train of propagating action potentials. Henceforth, we shall assume that the restitution functions  $f$  and  $c$  can be applied locally at each position  $x$  along the fiber.

By numerically solving Equations (1)–(2) we may graph  $v(x, t)$  versus  $x$  and  $t$ , yielding a surface in three-dimensional space (Figure 2, left). Taking the intersection of this surface with the plane  $v = v_{\text{thr}}$  generates a sequence of curves which we identify with the wave fronts and wave backs of the action potentials. Projecting these curves onto the  $xt$  plane yields a schematic space-time plot of the wave fronts and wave backs as illustrated in the right panel of Figure 2. Here,  $\phi_n(x)$  and  $\beta_n(x)$  denote the times at which the  $n$ th wave front and wave back (respectively) arrive at  $x$ .

To construct the portrait of wave fronts and wave backs, suppose that  $D_{n-1}(x)$  is known. Pacing with period  $B$  at  $x = 0$  imposes the requirement that  $\phi_n(0) = n \cdot B$ . Therefore, we may determine  $\phi_n(x)$  by integrating

$$\frac{d\phi_n}{dx} = \frac{1}{c(D_{n-1}(x))}, \quad \phi_n(0) = n \cdot B. \quad (8)$$

Equation (8) uses the fact that the inverse of the slope of the curve  $\phi_n(x)$  is equal to the wave front velocity which, by assumption, can be expressed in terms of the preceding DI. The wave back  $\beta_n(x)$  is obtained immediately:

$$\beta_n(x) = \phi_n(x) + A_n(x) = \phi_n(x) + f(D_{n-1}(x)), \quad (0 \leq x \leq L). \quad (9)$$

To determine the next pair  $\phi_{n+1}(x)$ ,  $\beta_{n+1}(x)$ , we must first solve for  $D_n(x)$ . To do so, observe that  $D_n(x) = \phi_{n+1}(x) - \beta_n(x) = \phi_{n+1}(x) - \phi_n(x) - f(D_{n-1}(x))$ . Differentiating with respect to  $x$  and defining  $G(DI) = c(DI)^{-1}$  for notational convenience, we obtain a new initial value problem

$$\frac{dD_n(x)}{dx} = G(D_n(x)) - G(D_{n-1}(x)) - \frac{d}{dx}f(D_{n-1}(x)), \quad (10)$$

$$D_n(0) = B - f(D_{n-1}(0)). \quad (11)$$

Solving this system for  $D_n(x)$ , we are able to determine both  $\phi_{n+1}(x)$  and  $\beta_{n+1}(x)$ . Given  $D_0(x)$ , we may solve (10)–(11) recursively for  $n \geq 1$ .

### 2.4 Solution of the linearized equations

The linearization of Eqs. (10)–(11) can be solved exactly (see [1] for additional detail). To do so, let  $D^*$  denote the steady-state DI associated with long-term pacing with period  $B$ , and let  $y_n(x)$  denote our approximation of  $D_n(x) - D^*$ .

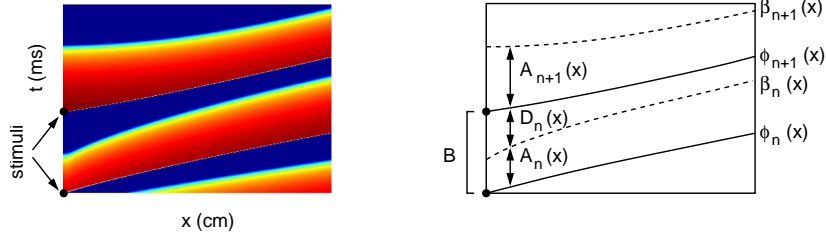


Figure 2: Left: Solution of (1)–(2) for particular parameter choices. Right: The corresponding wave fronts (solid curves) and wave backs (dashed curves).

In particular,  $y_0(x) = D_0(x) - D^*$ . For  $n > 0$ , the linearization of Eqs. (10)–(11) about  $D^*$  is given by

$$\frac{d}{dx} [y_n(x) + \alpha y_{n-1}(x)] = -\lambda [y_n(x) - y_{n-1}(x)], \quad (12)$$

$$y_n(0) = -\alpha y_{n-1}(0), \quad (13)$$

where

$$\alpha = f'(D^*) \quad \text{and} \quad -\lambda = G'(D^*). \quad (14)$$

As shown in [1], one may rearrange (12)–(13) and use an integrating factor to solve for  $y_n(x)$  in terms of  $y_{n-1}(x)$ , obtaining the recursive sequence

$$y_n(x) = -\alpha y_{n-1}(x) + (\alpha + 1)\lambda \int_0^x e^{-\lambda(x-s)} y_{n-1}(s) ds, \quad (n \geq 1). \quad (15)$$

To facilitate the solution of (15), introduce the operator  $T = -\alpha I + (\alpha + 1)\lambda K$  on the Banach space  $(C[0, L], \|\cdot\|_\infty)$ , where  $I$  is the identity operator and

$$(K\varphi)(x) = \int_0^x e^{-\lambda(x-s)} \varphi(s) ds. \quad (16)$$

Clearly  $y_n = T y_{n-1} = T^n y_0$ , which suggests that we must compute powers of the operator  $T$ . The details of this calculation appear in [1], where it is shown that  $T^n$  can be expressed in terms of a convolution

$$(T^n \varphi)(x) = (-\alpha)^n \varphi(x) + \int_0^x \Psi_n(s) \varphi(x-s) ds. \quad (17)$$

The kernel  $\Psi_n$  is given by

$$\Psi_n(s) = (-\alpha)^{n-1} (\alpha + 1) \lambda e^{-\lambda s} L_{n-1}^{(1)} \left( \frac{\lambda(\alpha + 1)s}{\alpha} \right), \quad (18)$$

where  $L_{n-1}^{(1)}$  is a *generalized Laguerre polynomial* (see Szegő [8]). For emphasis, we remark that the solution of the linearized kinematic model is given by  $y_n(x) = (T^n y_0)(x)$ , where  $y_0$  is obtained from the initial profile of DI values.

### 3 Discussion

The kinematic model (10)–(11) is far more computationally efficient than the underlying reaction-diffusion model (1)–(2). For example, we compared the time required for numerical simulation 10 action potentials, using a Crank-Nicolson solver, a fiber of length  $L = 10$  cm, a spatial step of  $\Delta x = 0.01$  cm, and a time step of  $\Delta t = 0.01$  ms. Simulations with the kinematic model were over 1000 times faster than the reaction-diffusion model. Moreover, it is especially encouraging to note that even the solution of the *linearized* kinematic model (17) exhibited surprisingly good agreement with the simulations of the full reaction-diffusion model (see, for example, Figure 4 of [1]).

Of course, kinematic models have several serious drawbacks. First, by only following the progress of each action potential, the kinematic model does not possess the level of physiological detail of a standard reaction-diffusion model. Second, our assumption that  $f$  and  $c$  can be applied locally is only valid in certain physiological regimes. Finally, we remark that the spectrum of the operator  $T$  is given by  $\sigma(T) = -\alpha$ , where we recall that  $\alpha$  is the slope of the restitution function  $f$  at  $D^*$ . Therefore, if  $\alpha > 1$ , we would expect  $\|T^n\| \rightarrow \infty$  as  $n \rightarrow \infty$ , and our analysis of the linearized system no longer applies.

### References

- [1] J.W. Cain, Dynamic behavior of a paced cardiac fiber, *SIAM J. Appl. Math.*, **66** (2006), 1776–1792.
- [2] J.W. Cain, D.G. Schaeffer, Two-term asymptotic approximation of a cardiac restitution curve, *SIAM Review*, **48** (2006), 537–546.
- [3] J.W. Cain, E.G. Tolkacheva, D.G. Schaeffer, D.J. Gauthier, Rate-dependent propagation of cardiac action potentials in a one-dimensional fiber, *Phys. Rev. E*, **70** (2004), 061906.
- [4] J.P. Keener, J. Sneyd, *Mathematical Physiology*, Springer-Verlag, New York (1998).
- [5] C.C. Mitchell, D.G. Schaeffer, A two-current model for the dynamics of cardiac membrane, *Bull. Math. Bio.*, **65** (2003), 767–793.
- [6] J.B. Nolasco, R.W. Dahlen, A graphic method for the study of alternation in cardiac action potentials, *J. Appl. Physiol.*, **25** (1968), 191–196.
- [7] J. Rinzel, K. Maginu, Kinematic analysis of wave pattern formation in excitable media, In: *Non-Equilibrium Dynamics in Chemical Systems*, A. Pacault and C. Vidal, ed., Springer-Verlag, Berlin (1984).
- [8] G. Szegő, *Orthogonal Polynomials, 4th Edition*, AMS, Providence (1975).